

FEM analysis of behaviour of a geogrid reinforced soil slope with a complex geometry

Q. Napoleoni, V. Mencaccini

Dept. Hydraulics Transportation and Roads, Faculty of Engineering, University of Rome "La Sapienza", Rome, Italy

P. Rimoldi

Tenax SpA, Geosynthetics Technical Office, Milan, Italy

Keywords: Numerical modelling, Case study, Slopes, Reinforcement, Geogrids

ABSTRACT: One of the situations where reinforced soils (with a vegetated face) find their most pregnant use is the restoration of failed slopes. This kind of situation occurred in the town of Montone, in the province of Perugia in Central Italy. A failed slope along a road, 15 m high, was reconstructed with a geogrid reinforced soil designed with three steps, each about 5 m high, with two horizontal berms between them. Monodirectional HDPE extruded geogrids were used to reinforce the slope. The construction was carried out using permanent steel meshes as formworks to support the face. In 1993, for research purposes, a section of the slope was instrumented with strain gauges on the geogrids and total pressure cells at the base. In situ and laboratory tests yielded the value of the deformability and resistance characteristics of the soil and of the geogrids. Data derived from the above measurements allowed to perform a FEM back-analysis of the behaviour of the reinforced soil slope. The paper reports about the method and results of the FEM analysis.

1 INTRODUCTION

Within the several types of technology used for constructing reinforced soil, those ones that permit the achievement of a fully vegetated face play a very important role. One of the design situations where the latter technologies are largely used is the restoration of failed slopes. The use of reinforced soil actually permits the reconstruction of such slopes, with geometry close to the original, by using the same soil of the landslide, with minimised environmental impact. Moreover a considerable economic saving can be achieved compared to the most common solution which uses soil with better mechanical characteristics, excavated in other locations and transported to the work site. This type of earthwork was carried out in the town of Montone, in the province of Perugia in Central Italy (Coluzzi et al. 1997).

Such project is atypical since:

- The reconstruction of the slope was carried out by constructing a geogrid reinforced steep slope, composed of three steps, each about 5 m high and with the face at 60° inclination, in alternation with two horizontal berms (Fig. 1);
- For research purposes, a section of the reinforced slope was instrumented by means of strain gauges applied to the geogrids and total pressure cells installed at the base of the slope;
- By tests performed both in situ on the structure and in laboratory on soil and geogrid samples taken from the structure, the main physical-mechanical parameters of the two materials were determined.

It was thus possible to study the behaviour of the reinforced soil structure by finite elements numerical modelling. In order to investigate the real behaviour of reinforced soil in a case characterised by a relatively complex geometry.

2 DESCRIPTION OF THE STEEP REINFORCED SLOPE

In order to stabilise the slope, it was decided to reconstruct the slope by means of a reinforced soil slope, with monodirectional HDPE extruded geogrids as reinforcement. The slope had a height of 15.50 m and was subdivided into three steps, having heights of 5.30 m, 5.60 m and 4.60 m, in alternation with two horizontal berms of 4.10 m and 3.10 m in width, for a total running length of about 50 m. The face had a 60° inclination with respect to the horizontal plane (Fig. 1). The reinforced slope was constructed by using the debris taken from the landslide body, plus minor quantities of other materials from nearby quarries. To perform the work, 23 layers of reinforcement were used. These were placed at vertical centres of 0.65 m, with variable lengths between 3.15 m and 4.5 m (Fig. 1).

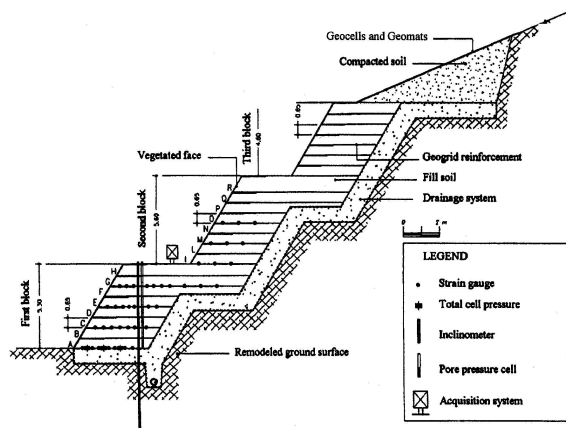


Figure 1. Cross-section of the instrumented reinforced soil slope (Ghinelli and Sacchetti 1998).

Each step of the reinforced slope was designed using the Jewell method (Rimoldi et al. 1997). In designing the single steps, the problem arose that the top of the slope was not flat, which is a requirement for applying the Jewell method (Jewell 1989). This was taken into account by using vertical, fictitious surcharges. These vertical surcharges differed for the three steps. In particular, surcharges of 7 kPa for the lower step, 40 kPa for the central step and 20 kPa for the upper step were used.

With regards to reinforcement, the result of the calculations showed the suitability of a monodirectional HDPE extruded geogrid, with mechanical characteristics shown in Table 1.

Table 1. Mechanical properties of the geogrid (Tenax TT060 Samp)

Peak tensile strength	kN/m	60
Strength at 2% strain	kN/m	17
Long term design strength	kN/m	25

2.1 Construction of the reinforced slope

The reinforced slope was constructed by using the “wrap-around” technique with permanent welded wire mesh formworks for supporting the face (Fig. 2). This method permits reinforced soil slopes to be made with a vegetated face having up to 70°-80° inclination.

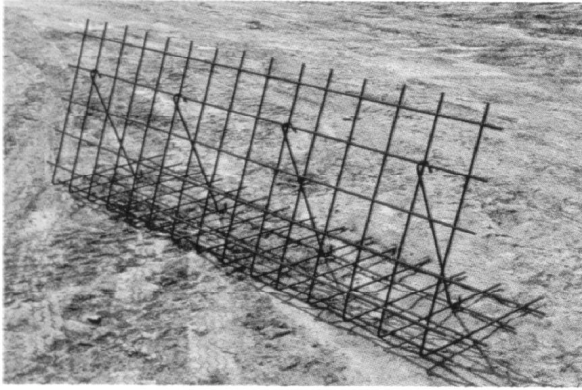


Figure 2. Permanent welded wire mesh formworks.

The use of such formworks helps in constructing the face of the slope and permits to obtain a uniform inclination. The form-works are obtained through the mechanical folding of steel wire mesh sheets (mesh: 150 x 150mm; $\varnothing = 8\text{mm}$) and are equipped with suitable connecting hooked rods that guarantee geometric stability of the formworks themselves, even during the compaction of the soil (Fig. 2).

On the inside, between the geogrid and the soil, a biomat was placed. Its function is to protect the face from the erosive activity of atmospheric agents and to form an appropriate surface on which the hydro-seeding of suitable herbaceous essences can be made.

Figure 3 illustrates the reinforced slope at the completion of construction: metallic and synthetic elements are very evident at the face.



Figure 3. View of the reinforced slope in Montone at completion of construction (Coluzzi et al. 1997)

2.2 Measurements

For research purposes, a section of the slope was instrumented by means of strain gauges applied to the ribs of the geogrids, and total pressure cells placed at the base of the first step (Coluzzi et al. 1997). The strain gauges were placed on the geogrids with the aim of measuring the distribution of the longitudinal deformations along the grids themselves. In particular, the first, third and fifth geogrid layers of the first step were measured by positioning the strain gauges at 0.50 m, 1.00 m, 1.50 m, 2.00 m, 2.50 m, and 3.00 m from the face; the seventh geogrid of the first step was measured by positioning the strain gauges at 0.50 m, 1.00 m, 1.50 m, 2.00 m, 2.50 m, 3.00 m, 3.50 m, 4.50 m, 5.50 m and 6.50 m from the face; the first, third and fifth geogrids of the second step were measured by positioning the strain gauges at 0.50 m, 1.00 m, and 1.50 m from the face (Fig. 1).

The total pressure cells were placed at the base of the first step to be able to establish the real distribution of vertical pressures. In particular, they were positioned at 1.00 m, 2.00 m and 3.00 m distance from the face (Fig. 1).

2.3 In situ and laboratory geotechnical tests

As mentioned previously, once the reinforced slope has been constructed, in situ geotechnical tests on the structure and lab tests on samples of soil taken from the same slope were performed (Sacchetti 1998).

In particular: in situ density tests on the three steps with the aim of evaluating the effective degree of compaction of the soil; load tests on circular plates ($D = 300$ mm and 600 mm) on the first step with the aim of evaluating the deformation parameters of the fill; direct shear tests on samples reconstructed with the soil taken in situ aimed at determining the strength characteristics of the fill.

3 FINITE ELEMENTS MODELLING

Ghinelli and Sacchetti (1998) published a first numerical modelling of this reinforced slope. This modelling, made by means of CRISP 90 code, used the following basic elements and relative constitutive laws:

- Bar elements with linear, elastic behaviour for modelling the reinforcement;
- Triangular and quadrilateral elements with perfectly elastic-plastic behaviour for modelling the fill;
- SLIP elements with behaviour based on the Goodman and Taylor model (1968) for modelling the soil-reinforcement interface;
- Triangular and quadrilateral elements with elastic behaviour for modelling the foundation soil and the original soil of the slope behind the reinforced soil blocks.

The SLIP elements are particularly interesting: they are elements with a zero thickness and were used to simulate the complex phenomena of interaction at the interface between the soil and reinforcement. In fact, they are able to simulate an interface that is either almost perfectly smooth or rough and/or cohesive, further permitting the simulation of a relative movement among adjacent elements.

In the above mentioned modelling, there is no allowance for the presence of the steel wire meshes placed at the face. The presence of this formwork certainly influences the trend of the deformations, at least in the front area, by conditioning the trend of the deformability.

Other limitations of this model are:

- the use of a single constitutive law for the fill, which is actually composed of two very different materials (morainic soil for the fill and gravel for the drainage layers);
- the use of a single soil density for the three steps (in fact, different values for the three steps were obtained from the in situ density tests);
- the value of the stiffness of the geogrids is greater than the value normally used in presence of creep and in the range of measured deformations (around 900 kN/m);

Based on the above, a new numerical model was developed that, at least partially, could overcome these evident limitations. This was done by means of the SIGMA/W code developed by GEO-SLOPE. In constructing the mesh of the finished elements, the following criteria were followed:

- the real geometry of the reinforced slope and the drainage layers, as well as the exact location of the reinforcements, were respected.
- quadrilateral and triangular elements were used having a form that guarantees good numerical performance.
- with the aim of reducing the number of nodes employed and thus the computational load, a more “closely woven” mesh was used to outline those volumes of soil that were of particular interest, while a “larger” mesh was used for the rest of the model.
- with this same aim in mind, elements with secondary nodes were used only to model the volume of soil close to the face.
- A mesh composed of 1104 elements and 1058 nodes was obtained (Fig. 4).

The presence of geogrids was modelled by inserting elements called BAR into the mesh. These elements have an elastic behaviour and are endowed with extensional rigidity only. These are placed along the nodes of the mesh where the reinforcements are actually placed.

The presence of these elements implies that the displacements between the nodes tied by the BAR elements are conditioned among other things by their axial rigidity. The use of BAR elements implies the hypothesis that there are equal deformations in the soil and in the reinforcement: on the whole, it is assumed that relative soil-reinforcement movements are not possible. This hypothesis appears realistic if the reinforcement is a geogrid. In fact, the particles of soil get interlocked in the openings of the grid and consequently their movement is strictly conditioned by the geogrid itself (Fig. 5).

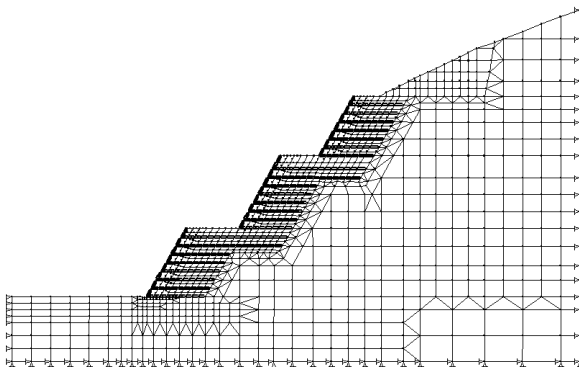


Figure 4. Finite Element Analysis Mesh

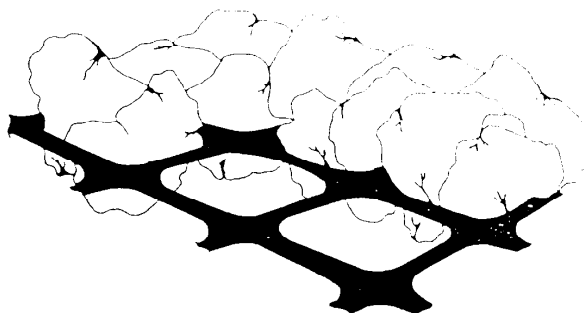


Figure 5. Interaction between soil and geogrid

Fannin and Hermann (1990) documented the validity of this assumption. They measured the behaviour a geogrid reinforced soil slope: both deformations in the geogrids and in the adjacent soil in various points have shown substantially equal values.

To model the presence of the steel mesh formworks, BEAM elements were used, namely, structural elements having an elastic behaviour with axial and bending rigidity. In order to respect the form of the steel wire meshes, these elements were placed along the facial nodes and, horizontally, for 500 mm along the plane of the reinforcement.

BEAM elements belonging to different layers were disconnected (Fig. 6).

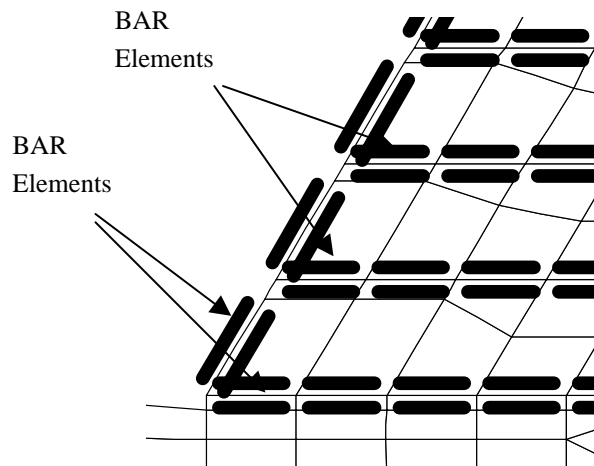


Figure 6. Details of the face area

Table 2 summarises the constitutive laws and the physical-mechanical parameters adopted for each type of material.

The in situ soil was modelled with a linear-elastic constitutive law. The deformability parameters (E and ν) were chosen in agreement with Ghinelli and Sacchetti (1998), so that the soil could constitute an adequate support for the reinforced soil. For the fill a perfectly elastic-plastic behaviour was adopted, considering valid the Mohr-Coulomb resistance criterion.

The values of deformability and resistance assigned to the drainage layer were estimated while those relative to the reinforced soil were obtained from the plate loading tests and direct shear tests. The unit volume weight assigned to the fill were those obtained from in situ density tests.

Table 2. Properties of the materials employed

Material	In situ soil	Drainage layer	Soil (1° step)	Soil (2° step)	Soil (3° step)
Constitutive law	Linear-elastic	Plastic-elastic	Plastic-elastic		
E (MPa)	10	40	35.2		
ν	0.4	0.33	0.2		
ϕ'	-	45	33		
c' (kN/m ²)	-	0	0		
γ (kN/m ³)	20	18.1	20.8	18.1	19.8

Regarding the stiffness of the reinforcements, the value $K=900$ kN/m was chosen. This value represents the short-term stiffness of the geogrid used if deformations are about 2%. This stiffness value could be too large if creep phenomena were to occur. Since creep phenomena relative to the

geogrids confined in the soil are not known with sufficient reliability, a decision was made to also perform an analysis using the value $K = 600 \text{ kN/m}$.

With regard to the deformability values assigned to the BEAM elements that simulate the presence of the steel wire mesh, reference was made to a $150 \times 150 \text{ mm}$ mesh, $\square = 8 \text{ mm}$ elements, stiffened by connecting rods.

The values used are reported in table 4. With the aim of best simulating the various construction phases of the work, the loads were applied by increments. The three slope steps were divided into 13 load steps, each of them corresponding to the two compaction layers of soil between two reinforcement layers.

Table 4. Deformability parameters assigned to the BEAM elements

Elastic modulus E (kN/m^2)	210×10^6
Moment of inertia per unit of breadth (m^4/m)	3×10^{-7}
Area per unit of breadth (m^2/m)	0.0006

4 RESULTS OF FEM ANALYSIS

An analysis of the values of the geogrids deformations, obtained from the numerical modelling, shows a substantial agreement with the corresponding values measured by the strain gauges. Only in local situations that are difficult to model, the numerical results differ from the measurements. For example, figure 7 re-ports the deformation values of the geogrids located on the first step measured by means of strain gauges compared to those calculated by means of numerical analysis. The values reported are calculated for both stiffness values of the reinforcement as above described. A satisfactory agreement in the deformation values can be seen between the numerical modelling and the measurements performed in situ. The geogrid at the base A and the geogrid G are exceptions. The model results follow the experimental measures on these geogrids qualitatively but not quantitatively. In particular, on geogrid G, the double peak of the deformations is reproduced. As it can be seen, the peak closest to the face and the one farthest away belong to the critical surface of the first and second step, respectively.

The values of geogrids A and G may be due to numerous factors that the numerical method cannot model.

In particular, at the base of the first step, the presence of a geotextile above the foundation drainage layer could strongly condition the deformations of geogrid A. In fact, the presence of this element may partially hinder the interlocking of the soil grains inside the geogrid holes. This implies that the geogrid-geotextile contact may constitute a surface of discontinuity on which small relative displacements may have occurred between the geogrid-fill structure and the geotextile-drain structure.

The numerical modelling of this aspect would require the use of elastic-plastic SLIP elements that are not available in the calculation code used.

Furthermore, the deformations of geogrid A are definitely influenced by the deformability characteristics of the drainage layer, which were not known.

With regard to geogrid G, the differences between the calculated and measured values may depend on local factors such as a different degree of compaction of the soil or the use of different materials in that area. In fact, slightly different types of soil were used in the construction of the reinforced slope. The soil particles distribution shows a rather large range, confirming that the fill was not uniform; moreover the following facts should be considered (Sacchetti 1998):

- different soil densities were measured on different steps;
- from the interpretation of different plate loading tests, carried out on the first step, different values of the deformation modulus were obtained.

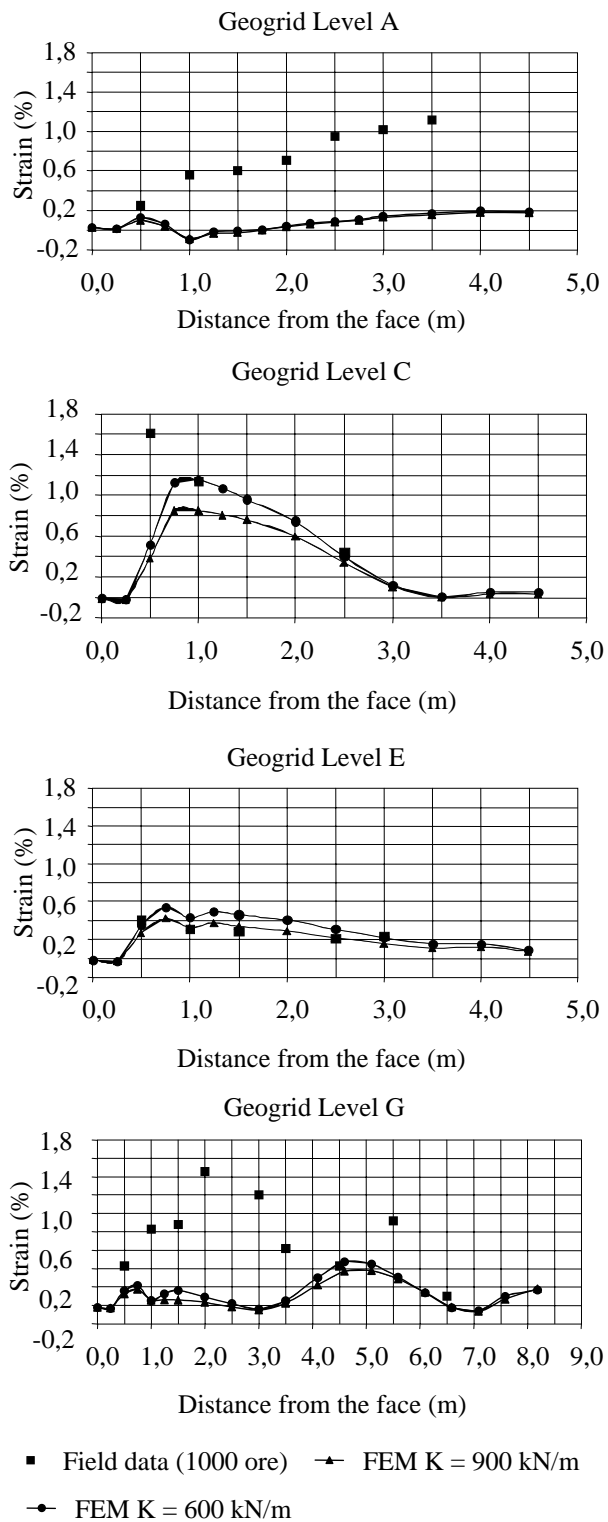


Figure 7. Deformations of the geogrids located on the first step: computed and measured values

Figure 8 shows a comparison among the maximum forces acting on reinforcements as determined through measurements, as determined through FEM modelling and as determined according to the Jewell method (1989). The first two types of forces were calculated by multiplying the maximum deformation of the geogrid (measured and calculated) by the stiffness of the geogrid. The forces according to the Jewell method (1989) were calculated as following: in one case no surcharge was applied, while a uniformly distributed surcharge of 70 kPa was applied in the other case (as done at the design stage).

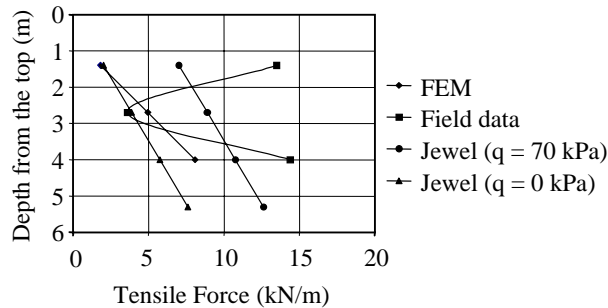


Figure 8. Maximum tensile forces in the geogrids of the first step obtained by different methods

Since, the surcharge is present only in the second step, and therefore is not distributed everywhere, one can state that the logic with which the SIGMA/W code distributes the values of maximum force follows that of the Jewell method.

From this viewpoint, it seems correct to attribute the high deformation values measured on geogrid G to local factors.

Figure 9 also shows a good agreement between the total vertical stresses at the base calculated by the model and the stresses measured by the total pressure cells.

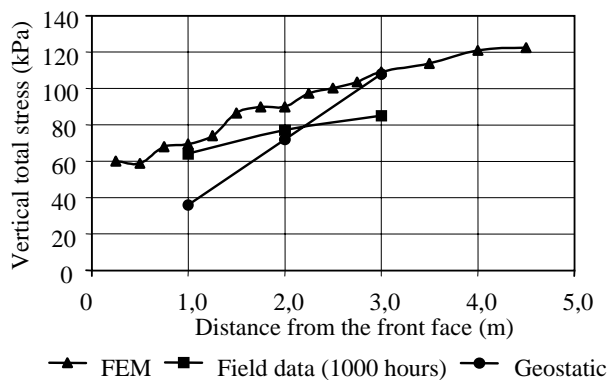


Figure 9. Comparison of the total vertical stresses at the base of the first step

Figures 10 and 11 represent the deformation of the reinforced soil slope at the end of the construction of the first step and at the end of construction, respectively. It is interesting to follow the evolution of the deformations of the soil and of the face during the various construction phases of the work. Figure 10 shows that the step tends to bulge in the lower part. This overall movement leads to an inward rotation of the face at the top of the step. Therefore that the part of the soil placed on the top of the step is slightly compressed against the existing slope. As the construction proceeds, the thrusts of the soil tend to push outward the higher volumes of the first step. At the

end of the construction of the second step, there are no horizontal displacements of the face, at the top of the first step, while the compressed volume is considerably reduced. At the completion of the construction of the whole slope, the entire face of the first step shows outward displacements (Fig. 11).

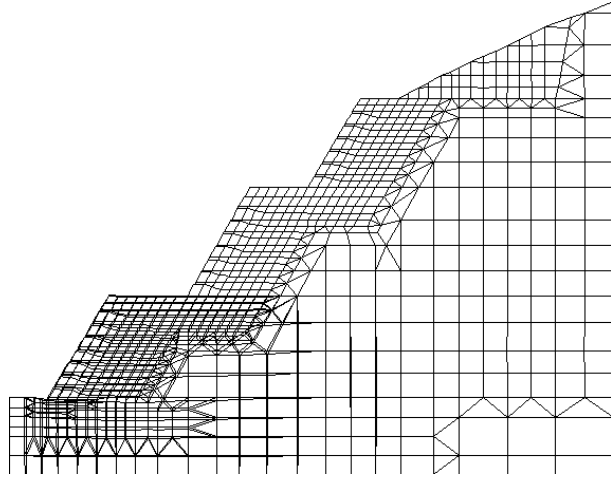


Figure 10. Deformation of the slope at the end of construction of the first step ($K = 900 \text{ kN/m}$)

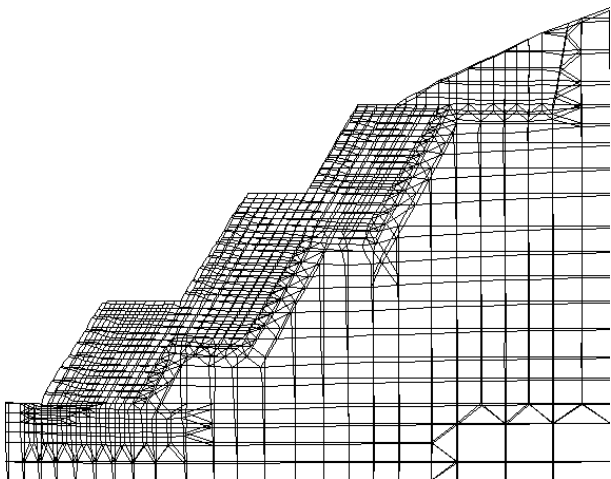


Figure 11. Deformation of the slope at the end of construction ($K = 900 \text{ kN/m}$)

Figure 12 reports the locations of the points in the soil that have equal horizontal deformations. As it can be seen, horizontal deformations tend to concentrate inside the soil, but not at the face. The result is that the face of the slope is subject to displacements, due to the global movements of the reinforced blocks, but not to distortions. This aspect can certainly be attributed to the presence of a considerably rigid element such as the steel wire mesh. This is confirmed in Figure 13 which shows the result of the analysis if the presence of the steel wire mesh is not modelled by means of BEAM elements. A generally larger level of deformations can be seen at the face. These deformations tend to be concentrated at midpoint between the layers. Thus deformation of the face presents larger displacements in the centre of the layers than those on the adjacent geogrids.

On the whole, the face is deformed like a catenary. An investigation of the site in Montone (and in other sites where reinforced slopes were constructed using the same technique) pointed out that the catenary type of deformation is not the one that exists in reality in this kind of structures. In fact, the deformation of reinforced slopes with permanent formworks has a quite regular distribution, without bulges at the centre line of the layers.

On the other hand, a catenary deformation of the face occurs in reinforced slopes constructed with temporary formworks, which are removed when a wrap-around layer is finished.

Looking at the isostrain curves, it is possible to draw the curves of maximum tensile forces in the geogrids. Such curves were obtained for the first two steps (Figure 12).

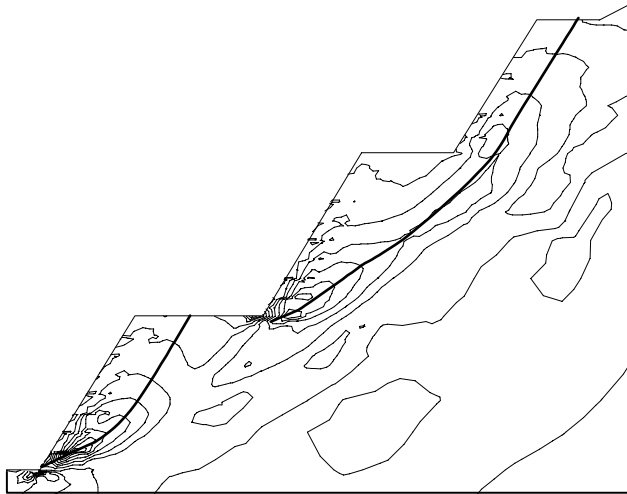


Figure 12. “Isostrain” curves and curves of maximum tensile forces in the geogrids ($K = 900 \text{ kN/m}$)

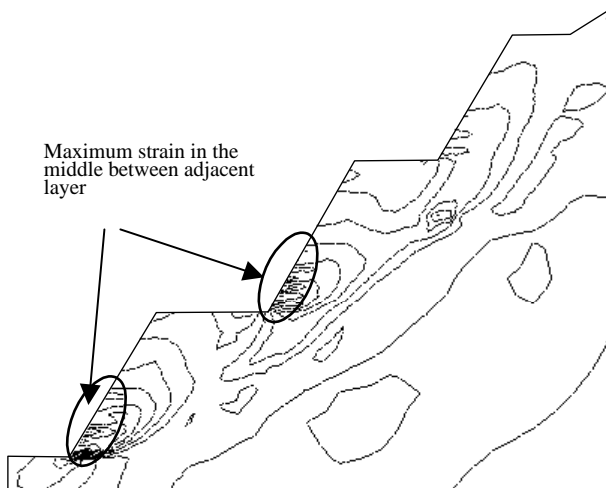


Figure 13. “Isostrain” curves obtained for the same slope but without the presence of the steel wire mesh ($K = 900 \text{ kN/m}$)

In the first step, the curve of the maximum tensile stresses confirms what is already known about reinforced soil slopes, composed of a single step and placed on firm soil: the points of the geogrids where the maximum tensile forces are localised are placed along a curvilinear surface

starting from the toe of the slope. The locus of the maximum tensile forces relative to the second step does not pass through its toe. It passes inside the first step and affects the upper geogrids. Thus the rear portions of said geogrids concur considerably to the stability of the second step

5 CONCLUSIONS

From the numerical analysis of the reinforced slope in Montone, the following conclusions can be drawn:

- A satisfactory agreement can be obtained between the experimental data and the results of the numerical modelling, except for local situations that are difficult to model. This confirms the validity of the FEM modelling technique in determining the complete deformative and tensional state inside a reinforced soil slope, even when the geometry is rather complex.
- To obtain a correct modelling of the problem, it is important to use a calculation code which permits the use of several types of elements and constitutive laws. In particular, SLIP elements having an elastic-plastic behaviour seem necessary to model the surfaces where relative displacements could occur.
- It is essential to model properly the permanent formworks. Modelling techniques that neglect the presence of this rigid element at the face are only suitable for reinforced soil structures that use temporary, removable formworks.
- The maximum tensile forces curve in the first step starts from the toe of the slope. But in the second step, it affects the geogrids along the lower step.
- The forces applied to the geogrids in each step increase linearly with the distance between the geogrid and the crest of the step.
- The values of the maximum forces in the geogrids of the first step, calculated by the numerical methods, substantially agree with those obtained using the Jewel method (1989), even though the Jewel method (1989) provides for cases of zero surcharge or of uniformly distributed surcharge on the crest of the slope, while in the present case the surcharge is distributed only on part of the top of the first step.

REFERENCES

- Coluzzi, E., Montanelli, F., Recalcati, P., Rimoldi, P., Zinesi, M. 1997. Preliminary results from an instrumented geogrid reinforced slope for the stabilisation of Montone hill in central Italy. Proc. International Symposium on Mechanically Stabilized Backfill (MSB): 307-314. Colorado (USA).
- Ghinelli, A., Sacchetti, M. 1998. Finite element analysis of instrumented geogrid reinforced slope. Proc. of the 6th International Conference on Geosynthetics: 649, 654. Atlanta (USA).
- Jewell, R.A. 1989. Theory of reinforced walls: revised design charts for steep reinforced slopes. Proc. of the conference reinforced embankments, theory and practice in the British Isles: 1-30. Cambridge (UK).
- Fannin, R. J., Hermann, S. 1990. Performance data for a sloped reinforced soil wall. Canadian Geotechnical Journal (1992): 676-686.
- Sacchetti, M. 1998. Analisi del comportamento tensio-deformativo nel tempo di geosintetici ad alta resistenza. PhD Thesis. University of Florence. (Italy).
- Rimoldi, P., Recalcati, P., Coluzzi, E. 1997. Un esempio di terre rinforzate con geogriglie: il consolidamento del colle di Montone (PG). L'Ingegnere e l'architetto (9/12/97):105-111. (Italy).